

PyRCN: Exploration and Application of ESNs

Peter Steiner^{*†}, Azarakhsh Jalalvand^{*‡}, Simon Stone[†], Peter Birkholz[†]

[†]Institute for Acoustics and Speech Communication
Technische Universität Dresden, Dresden, Germany

Email: peter.steiner@tu-dresden.de

[‡]IDLab, Ghent University – imec, Ghent, Belgium

Email: azarakhsh.jalalvand@ugent.be

Abstract—As a family member of Recurrent Neural Networks and similar to Long-Short-Term Memory cells, Echo State Networks (ESNs) are capable of solving temporal tasks, but with a substantially easier training paradigm based on linear regression. However, optimizing hyper-parameters and efficiently implementing the training process might be somewhat overwhelming for the first-time users of ESNs. This paper aims to facilitate the understanding of ESNs in theory and practice. Treating ESNs as non-linear filters, we explain the effect of the hyper-parameters using familiar concepts such as impulse responses. Furthermore, the paper introduces the Python toolbox PyRCN (Python Reservoir Computing Network) for developing, training and analyzing ESNs on arbitrarily large datasets. The tool is based on widely-used scientific packages, such as numpy and scipy and offers an interface to scikit-learn. Example code and results for classification and regression tasks are provided.

Index Terms—Reservoir computing, echo state networks, scikit-learn, PyRCN.

I. INTRODUCTION

Echo State Networks (ESNs) [1] are a special kind of Recurrent Neural Networks (RNNs). Although they are not as widely known as other types of RNNs, such as LSTM networks, they have achieved comparable results to typical deep-learning architectures in several recognition tasks, for example in speech, image, radar and music data processing [2]–[5].

The basic idea of ESNs is rather simple: The input features are sparsely connected to a pool of randomly connected non-linear neurons, the so called “reservoir”. Only connections from this reservoir to the output are trained, typically using linear regression. However, several hyper-parameters need to be tuned task-dependently in order to achieve optimal results. This requires serious trial and error, as mentioned for example in [6]. A current trend is to optimize hyper-parameters “blindly” using random optimization methods, such as Bayes Optimization [7]. However, as the hyper-parameters of ESNs have certain characteristics, understanding these might prevent from a naive random search with hundreds or thousands of evaluations. In this paper, we specifically analyze the properties of the most important hyper-parameters by treating the ESN as a non-linear recursive filter as Herbert Jaeger has proposed in [8]. Using impulse responses, we show how the individual hyper-parameters and their combinations influence the individual

impulse responses of the neurons inside the reservoir and thus the output of the network.

Several toolboxes have been developed in the past to develop, train, and evaluate ESNs. Herbert Jaeger published an extensive MATLAB[®] toolbox, called ESNTtoolbox¹ with example code for different benchmark tests. However, it has its own data format that is not compatible with the typical input and output data structure for MATLAB’s Deep Learning Toolbox, which practitioners would be used to. Since it was last updated in the year 2009, it is quite out-of-date. The more recent DeepESN toolbox for MATLAB[®] by Gallicchio and Pedrelli [9] is more modern, but still lacks an API that is compatible with other established toolboxes. This makes it difficult to slot an ESN into an existing processing pipeline to contrast and compare its performance with other models.

In the Python world, one of the most advanced toolboxes was OGER [10] that contained a lot of modules for Reservoir Computing, not only for ESNs. However, OGER was based on Python 2, which has reached its end of life in 2020. As a result, many of the packages used in OGER are not maintained anymore and its development stopped around the year 2013. There exist two follow-up projects of the OGER toolbox: the recently introduced ReservoirPy [11], and EchoTorch [12], a PyTorch implementation of ESNs. Both are actively developed. However, they share the disadvantages of the MATLAB[®] implementations introduced before as they both do not utilize any standard API and common data structures. Thus, it is difficult to get started with these implementations, or to insert an ESN into an existing pipeline.

With this paper, we introduce PyRCN (Python Reservoir Computing Network), a new toolbox for ESNs that is based on widely used scientific Python packages, such as numpy or scipy, and with an interface to the popular machine learning platform scikit-learn [13]. This makes it possible to use a lot of features from scikit-learn, such as cross-validation schemes and methods for hyper-parameter optimizations. The API is widely used and makes it possible to easily compare ESNs with built-in estimators, such as multilayer perceptrons (MLPs), without changing many lines of code or the dataset handling. Up to this point, we decided not to provide an interface to a deep-learning framework, because, as was mentioned above,

This research was financed by Europäischer Sozialfonds (ESF), the Free State of Saxony (Application number: 100327771) and Ghent University.

^{*}Equal contribution

¹<https://www.ai.rug.nl/minds/uploads/ESNTtoolbox.zip>

the training procedure of ESNs is considerably different from typical deep-learning models.

The remainder of this paper is structured as follows: in Section II, we briefly review the basic concepts of Echo State Networks and introduce our toolbox PyRCN. Section III describes the impact of different hyper-parameters on the Echo State Network. In the Sections IV and V, we quickly recapitulate several Regression and Classification tasks by the authors, using the toolbox. Finally, we summarize our work and give outlook into future work in Section VI.

II. ECHO STATE NETWORKS

A. Basic Concepts

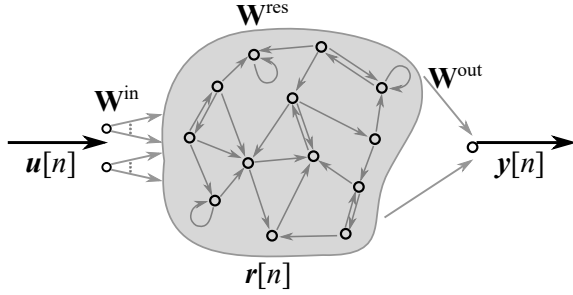


Fig. 1: Main components of an ESN: The input features are fed into the reservoir using the fixed input weight matrix W^{in} . The reservoir consists of unordered neurons, sparsely interconnected via the fixed reservoir matrix W^{res} . The output $y[n]$ is a linear combination of the reservoir states $r[n]$ based on the output weight matrix W^{out} , which is trained using linear regression.

The main outline of an ESN is depicted in Fig. 1. It consists of the input weights W^{in} , the reservoir weights W^{res} and the output weights W^{out} . The input weight matrix W^{in} has the dimension of $N^{res} \times N^{in}$, where N^{res} and N^{in} are the size of the reservoir and dimension of the input feature vector $u[n]$ with the time index n , respectively. Typically, the values inside the input weight matrix are initialized randomly from a uniform distribution between ± 1 and afterwards scaled using the input scaling factor α_u , which is a hyper-parameter to be tuned. However, in case of large reservoir sizes N^{res} , this leads to a large number of connections and makes it computationally expensive to feed the feature vectors into the reservoir. In [14], it was shown that it is sufficient to have only a limited number of connections from the input nodes to the nodes inside the reservoir. We therefore connect each node of the reservoir to only $K^{in} (\ll N^{in})$ randomly selected input entries. This makes W^{in} very sparse and feeding the feature vectors into the reservoir potentially more efficient. If the input is one-dimensional, the input is usually fully connected to the reservoir.

The reservoir weight matrix W^{res} is a square matrix of the size N^{res} . Typically, the values inside the reservoir weight matrix are initialized from a standard normal distribution. Similar to the input weight matrix, we connect each node

inside the reservoir to a limited number of $K^{rec} (\ll N^{res})$ randomly selected other nodes in the reservoir, and set the remaining weights to zero. The Echo State Property (ESP) requires that the states of all reservoir neurons need to decay in a finite time for a finite input pattern. In order to fulfil the ESP, the reservoir weight matrix is normalized by its largest absolute eigenvalue to achieve a spectral radius $\rho = 1$, because it was shown in [1] that the ESP holds as long as $\rho \leq 1$.

Together, the input scaling factor α_u and the spectral radius ρ determine, how strongly the network relies on the memorized past inputs compared to the present input. They need to be tuned task-dependently.

With the two weight matrices W^{in} and W^{res} , the reservoir state $r[n]$ can be computed in the following way:

$$r[n] = (1 - \lambda)r[n - 1] + \lambda f_{res}(W^{in}u[n] + W^{res}r[n - 1] + w^{bi}) \quad (1)$$

Equation (1) is a leaky integration of the reservoir neurons, which is equivalent to a first-order lowpass filter. Depending on the leakage $\lambda \in (0, 1]$, a specific amount of the past reservoir state is leaked over time. Together with the spectral radius ρ , the leakage λ determines the temporal size of the memory of the reservoir.

The reservoir activation function $f_{res}(\cdot)$ controls the non-linearity of the system. Conventionally, the sigmoid or tanh function is used, because their lower and upper boundaries ensure stable reservoir states. Every neuron inside the reservoir receives an additional constant bias input. The bias weights w^{bi} with dimension N^{res} are initialized by fixed random values from a uniform distribution between ± 1 and multiplied by the hyper-parameter α_b .

The output weight matrix W^{out} has the dimensions $N^{out} \times (N^{res} + 1)$ and connects the reservoir state $r[n]$, which is expanded by a constant intercept term of 1 for regression, to the output vector $y[n]$ using Equation (2).

$$y[n] = W^{out}r[n] \quad (2)$$

Typically, the output weight matrix is computed using ridge regression. Therefore, all reservoir states are concatenated into the reservoir state collection matrix R . As linear regression usually contains one intercept term, every reservoir state $r[n]$ is expanded by a constant of 1. All desired outputs $d[n]$ are collected into the desired output collection matrix D . Then, W^{out} can be computed using Equation (3), where ϵ is the regularization parameter that needs to be tuned on a validation set.

$$W^{out} = (RR^T + \epsilon I)^{-1} (DR^T) \quad (3)$$

The size of the output weight matrix $N^{out} \times (N^{res} + 1)$ determines the total number of free parameters to be trained in ESNs. Because linear regression can be obtained in closed form, ESNs are quite efficient and fast to train compared to typical deep-learning approaches.

An important extension to the basic ESN structure described so far are bidirectional ESNs.

Bidirectional ESNs: In the case of bidirectional ESNs, the feature vectors are first fed through the ESN as described above. Before the linear regression, the inputs are reversed in time, and again fed into the same reservoir. Afterwards, the reservoir states are again reversed in time to be chronologically aligned with the forward reservoir states. The reservoir state collection matrix \mathbf{R} is finally built by concatenating the states from the forward and backward pass. This doubles the number of free parameters for the linear regression. For example, the number of parameters for a reservoir with 500 reservoir neurons in the bidirectional case is $N^{\text{out}} \times (500 + 500 + 1)$, where 1 addresses the intercept term for linear regression.

B. PyRCN

In this section we introduce PyRCN, a light-weight and transparent toolbox to implement ESNs as described above and to address the disadvantages of many existing implementations. It is based on widely used scientific Python packages, such as numpy or scipy. We provide an interface to the popular machine learning platform scikit-learn [13], because it is widely used and depends on a minimal number of packages. Furthermore, it has a clear data structure and API, so that users of scikit-learn do not need to restructure their research data in order to use ESNs. Scikit-learn offers a lot of parameter optimization methods that can be utilized out-of-the-box.

Most of the existing ESN implementations usually collect the entire state collection matrix \mathbf{R} at once and then solve the linear regression to train ESNs. Especially for large datasets, this is not feasible on a normal computer. In PyRCN, we therefore offer an incremental training, which has two advantages: (1) It allows splitting very large datasets into subsets that fit into the available memory, and (2) it allows pausing the training entirely or adding more training data later, enabling the adaptation of the trained model to new circumstances.

All hyper-parameters introduced in Section II-A and more are included in the interface of PyRCN. Thus, users can easily explore the impacts and properties of different hyper-parameters. In the next section, we will use PyRCN to explore the most important hyper-parameters and their impact on the reservoir state. Furthermore, we will show the application of PyRCN on some example datasets for classification and regression tasks. The code examples for the experiments conducted in this paper are publicly available in our Github repository².

III. ESN ANALYSIS

In this section, we analyze the impact of the most important hyper-parameters, e.g. the input scaling α_u , the spectral radius ρ , the leakage λ and the bias scaling α_b . To that end, we feed a time-shifted unit impulse into a small ESN and observe the absolute values of the impulse responses inside the reservoir.

We use an ESN with $N^{\text{res}} = 50$ neurons, $K^{\text{in}} = 1$ and $K^{\text{rec}} = 10$ to work with a one-dimensional input. Every node

inside the reservoir receives the input and values from 10 randomly selected nodes in the reservoir.

A. Input scaling

To analyze the impact of the input scaling α_u , we supply the reservoir with an impulse at $n = 5$ with a non-zero value for the input scaling and neutralize the other hyper-parameters, i.e., no recurrent connections ($\rho = 0$), no bias ($\alpha_b = 0$) and no leakage ($\lambda = 1$). If we select an input scaling $\alpha_u = 0.1$, we can see in Fig. 2 that all reservoir states are zero all the times except for $n = 5$, when the impulse is fed into the ESN. Because we use random connections between ± 0.1 , the absolute values of the reservoir states remain from 0 to 0.1 (see Fig. 2 left). If we increase the input scaling to $\alpha_u = 1$, we can see in Fig. 2 right that each reservoir state still has only one non-zero value at $n = 5$ as before, just with higher activations up to 0.8. The tanh non-linearity is damping the reservoir states so that they cannot reach 1.

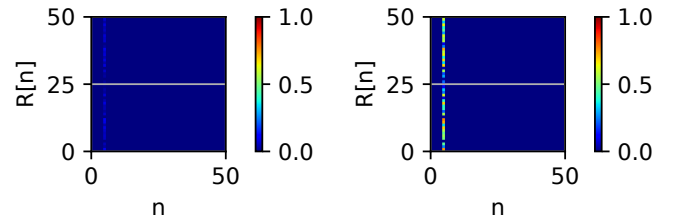


Fig. 2: Absolute values for the impulse responses of the reservoir neurons for different input scaling values. The left plot ($\alpha_u = 0.1$) shows a linear behavior in case of a small input scaling, whereas the right one ($\alpha_u = 1$) is damped non-linearly, due to the tanh non-linearity of the reservoir. Due to the absence of recurrent connections, all neurons have exactly one non-zero-state at $n = 5$.

B. Memory concepts and stability

As explained above, an ESN benefits from two different memory concepts, (1) recurrent connections controlled by the spectral radius ρ , and (2) leaky integration controlled by the leakage λ .

We begin with the spectral radius, one of the most important hyper-parameters of ESNs. As mentioned before, the reservoir weight matrix \mathbf{W}^{res} is scaled to have a unitary spectral radius. For the optimization, ρ can then be re-scaled to maximize the performance of a specific task. In the following experiments, the input scaling factor is fixed to $\alpha_u = 1$. At first, we increase the spectral radius to $\rho = 0.3$ and visualize the reservoir states in the top left plot of Fig. 3. We can observe that the impulse responses are starting at $n = 5$ and decaying until reaching zero after a short time. Obviously, the reservoir states are decaying rather fast, because the recurrent connections are small compared to the input scaling. If we increase the spectral radius to $\rho = 0.9$, we can see in the top right plot of Fig. 3 that the reservoir states are active over a longer time now ($n \approx 30$). Thus, we have an increased memory of the reservoir

²<https://github.com/TUD-STKS/PyRCN>

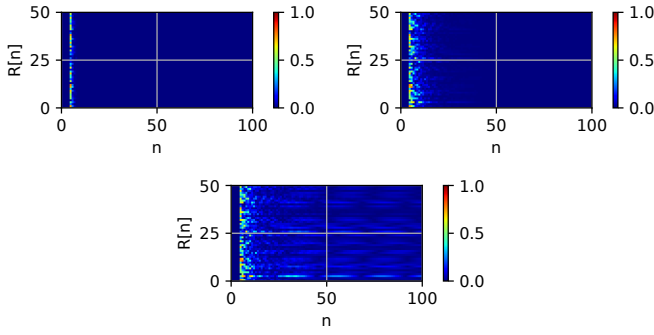


Fig. 3: Impulse responses of the reservoir neurons for different spectral radius. The top left plot for $\rho = 0.3$ shows that the reservoir activations are decaying rather fast. Around $n = 10$, they are almost zero. In the top right plot for $\rho = 0.9$, we observe that the reservoir states remain active longer as they are decaying until $n \approx 30$. In case of a spectral radius of $\rho = 1$ as in the bottom plot, the reservoir states are decaying not completely and start oscillating around $n \approx 25$.

here. It is important to notice that only a few neurons have high activations over a longer time, which is due to the sparse connections between the reservoir neurons. Every neuron in the reservoir receives information from just $K^{\text{rec}} = 10$ other neurons.

We can also visualize the impact of normalizing the reservoir matrix to the maximum absolute eigenvalue. The bottom plot of Fig. 3 shows the impulse responses for $\rho = 1$. We can see that the reservoir states are decaying very slowly, and they are oscillating with a resonance frequency. For many tasks, it is indeed necessary to preserve the echo state property of reservoir and keep $\rho < 1$. However in some cases, such as time-series prediction in this paper, the spectral radius can be larger than 1.

The second memory concept for Echo State Networks was introduced in [15]. The leaky integration with the hyper-parameter λ “leaks” a specific amount of the past reservoir state over time. In practice, this means that the reservoir state of each neuron will change faster or more slowly depending on the leakage λ . If we combine both memory concepts by having a non-zero spectral radius ($\rho = 0.9$) and a leakage that is smaller than one ($\lambda = 0.3$), we can observe in Fig. 4 that the leakage behaves in the same way for all nodes in the reservoir and acts like a low-pass filter. The magnitude is strongly damped, and all reservoir states are decaying exponentially over a longer time. Due to the spectral radius, all neurons have individual decaying times.

To summarize the different memory concepts: The recurrent connections enable the ESN to incorporate past information. Because every node is connected to a limited number of other nodes in the reservoir, many different relationships between the nodes can be learned. The leakage is a global memory scaling parameter and is responsible to smooth all reservoir trajectories.

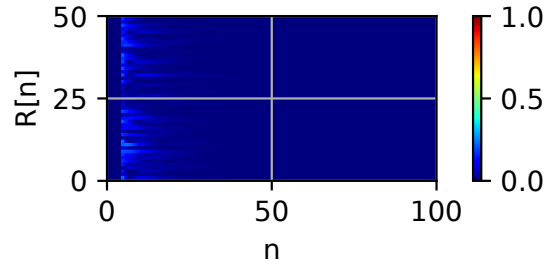


Fig. 4: Impulse responses for the spectral radius $\rho = 0.9$ and the leakage $\lambda = 0.3$. Due to the leakage, we can clearly observe that all impulse responses are low-pass-filtered. However, due to the spectral radius, each neuron has its specific decay time. Thus, the ESN is able to learn different time scales while still having rather smooth state transitions.

C. Bias

Another hyper-parameter to be studied is the bias scaling α_b . So far, we have noticed that the stable state of all reservoir neurons was the center value of the tanh activation function, i. e. 0, and that it is difficult to reach its boundaries (± 1). The bias scaling can help reach more non-linear areas of the activation function by changing the stable state of the reservoir nodes. This is useful for many classification tasks, which are rather non-linear.

In Fig. 5, we visualize the impact of $\alpha_b = 0.2$ without leaky integration ($\lambda = 1$) and with a spectral radius of $\rho = 0.9$. Two impacts of the bias scaling can be mainly observed:

- 1) The absolute value of the stable states of the reservoir neurons is approximately distributed from 0 to 0.2 and each neuron has its own stable state. When new information from the input is passed to the reservoir neurons, this is the excitation point.
- 2) Before the impulse arrives in the reservoir ($n = 5$), the states are approaching their stable state. Due to the spectral radius, each reservoir neuron is connected to other neurons and thus feeds the constant bias through the network, until each neuron has reached its final state.

For some tasks, such as time-series prediction, the observed “initial trajectory” [6] can be disadvantageous as it disturbs the first outputs. In that case, we can dismiss the first few reservoir states from the training.

IV. SOLVING REGRESSION PROBLEMS WITH ESNs

Due to their simple training procedure and architecture, ESNs are suitable for several regression tasks, especially for prediction of time-series. This can be done offline as well as online. In [16] for example, the authors used an Echo State network for online nonlinear prediction of speech using different numbers of past values. In [17], ESNs were used for stock price prediction. In [1], Jaeger showed that small ESNs can predict the Mackey-Glass time-series, a well-known benchmark test.

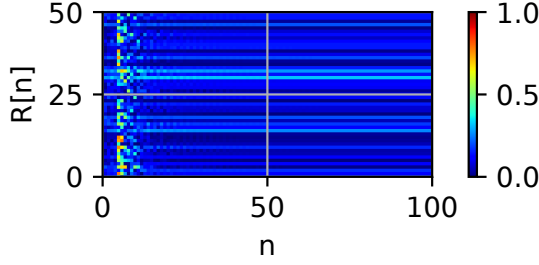


Fig. 5: Impact of the bias scaling $\alpha_b = 0.2$ on the impulse responses without leaky integration. We can clearly observe that each neuron needs some time in to reach their stable state before the impulse is fed into the reservoir. Without the impulse, the reservoir states reach a stable point after some time.

In the following, we present results for the Mackey-Glass benchmark and stock price prediction using the proposed PyRCN tool.

A. Mackey-Glass-Dataset

The Mackey-Glass system is essentially the differential equation in Eq. (4), where we set the parameters to $\alpha = 0.2$, $\beta = 10$, $\gamma = 0.1$ and the time delay $\tau = 17$ in order to have a mildly chaotic attractor.

$$\dot{y}(t) = \alpha y(t - \tau) / (1 + y(t - \tau)^\beta) - \gamma y(t) \quad (4)$$

In [1], a time-series with these parameters has been prepared, which we are using here. The first 500 samples are visualized in Fig. 6.

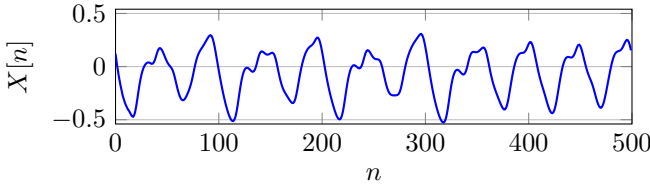


Fig. 6: The first 500 samples from the Mackey-Glass time-series.

Before we develop an ESN, we normalized the time-series to the range of ± 1 . Then, we extracted sub-sequences for training and testing the ESN. We used the 2000 first samples as a training sequence, and tested the ESN with the next 2000 samples, which were not used for training.

The ESN receives one sample at a time and needs to predict the next sample. Thus, we have a one-dimensional input and can set K^{in} to 1. As before, we can set $K^{\text{rec}} = 10$ to produce sparse reservoir connections. In order to tune the remaining hyper-parameters, we performed an exhaustive grid search across α_u , ρ , λ and α_b by minimizing the mean squared error

(MSE) between the predicted output and the original training sequence. This was done using scikit-learn's GridSearchCV.

The best hyper-parameters were $\alpha_u = 1$, $\rho = 1.2$, $\lambda = 1$ and $\alpha_b = 0$. The regularization parameter ϵ was fixed to 10^{-4} , and the reservoir had 500 neurons in total.

The lowest MSE obtained with this settings were 5.97×10^{-6} for the training set and 43.1×10^{-6} for the test set.

To briefly analyze the reservoir, we have visualized the impulse responses of the ten first reservoir neurons in Fig. 7.

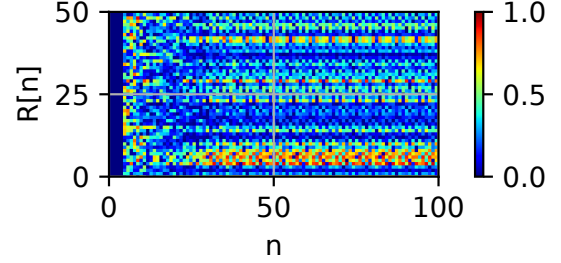


Fig. 7: Impulse responses for the ESN utilized for the Mackey-Glass task. We can see that the neurons activations have very strong transients in the beginning until they find an attractor and begin to oscillate more periodically.

When the impulse reaches the reservoir, we can see that many neurons are immediately excited relatively strongly. This is caused by the high input scaling of 1. Afterwards, until $n \approx 30$, the reservoir states behave strongly non-linearly, until they find an attractor and begin to oscillate more periodically. The chosen hyper-parameters give us two important insights:

- 1) The spectral radius can be larger than 1, as this is a generative and strongly non-linear task. Thus, the ESP can be violated for this kind of tasks.
- 2) The ESN with 500 free parameter needs, at least for this simple example, only 2000 training samples.

B. Stock Price Prediction

Another interesting task is stock price prediction and in this case, we predict a day's stock price based on the past information. Therefore, we have used the publicly available dataset "Gold Aug 20(GC=F)" in USD between 2000-02-28 and 2020-05-28 from <https://finance.yahoo.com>. It consists of several columns. Here, we just used the "Close" value, the final value of one day. We pre-processed the dataset by removing undefined values, namely, weekends and public holidays. The remaining values were normalized to be in a range of $[0, 1]$. They are visualized in Fig. 8 in blue. As one can see, the stock price trends upwards for the first few thousand days. Then goes down at around $n = 3300$ before climbing again after around $n = 4900$. The first 3000 values were used to train the ESN and to optimize the hyper-parameters and the rest for testing. Both, the input and output are one-dimensional and thus we use the global parameter $K^{\text{in}} = 1$ to fully connect the input to every neuron in the reservoir. Because we set

$K^{\text{rec}} = 10$, each neuron inside the reservoir received values from 10 other neurons. The total number of nodes in the reservoir was $N^{\text{res}} = 100$.

We performed an exhaustive grid search over the hyper-parameters α_u , ρ and α_b and obtained the most suitable values, e.g. an input scaling $\alpha_u = 0.6$, a spectral radius $\rho = 0.9$ and the bias scaling $\alpha_b = .$

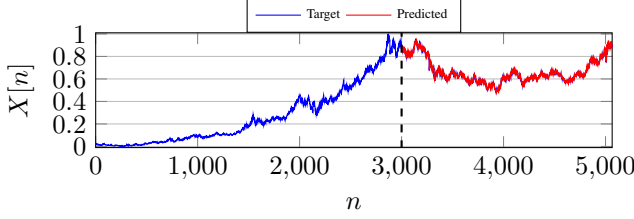


Fig. 8: Gold prices from the dataset “Gold Aug 20(GC=F)” in USD over a discrete time axis.

As before in the Mackey-Glass task, the resulting errors are quite low. The training MSE is 37.8×10^{-6} and the test MSE is 80.7×10^{-6} for the normalized time-series. In Fig. 8 we see that the ESN even captures the downward trend in the test set, although it has not seen any longer downward movement during the training.

V. CLASSIFICATION WITH ESNs

A. Multipitch Tracking in Music Signals

One rather challenging multilabel classification problem in music analysis is multipitch tracking, identifying all active notes or pitches present in an audio signal [5]. The challenges include:

- Unknown instruments: Even two different pianos have significant spectral differences
- Unknown polyphony: The number of active pitches at the same time is not constant and we do not know the maximum number.
- Wide pitch range: A piano, for example, has 88 different pitches. Other instruments can have even higher or lower pitches.

Here, we demonstrate how the ESN can deal with this challenging task. The approach is based on [5], but with different input features and using just one smaller reservoir instead of two very large ones. We use the MusicNet dataset [18] for training and evaluation, which consists of 320 audio files for training and a test set with 10 audio files. Sampled at a sampling frequency $f_s = 44\,100$ Hz, there are more than 30 h of annotated music. Due to this large amount of data, training a classifier is expensive in terms of time and memory consumption.

The acoustic features extracted from the input signal are obtained by filtering short-term spectra (window length 4096 samples and hop size 10 ms) with a bank of triangular filters in the frequency domain with log-spaced frequencies. The frequency range was 30 Hz to 17 000 Hz and we used 12 filters per octave. We used logarithmic magnitudes and added

1 inside the logarithm to ensure a minimum value of 0 for a frame without energy. The first derivative between adjacent frames was added in order to enrich the features by temporal information. Binary labels indicating absent (value 0) or present (value 1) pitches for each frame are assigned to each frame. Note that this task is a multilabel classification. Each MIDI pitch is a separate class, and multiple or no classes can be active at a discrete frame index.

The lengths of the feature vector and labels for each frame are 162 and 128, respectively. In total we have more than 12.1×10^6 frames for training. Assuming that the features are stored with standard float64 values, alone these need in total 15.8 GB memory. Thus, one can notice that this hardly fits into memory at once. In addition, we need to collect the reservoir states and compute the output weights. Many ESN implementations require all data to be loaded into memory at once. This makes it impossible to scale them for large datasets, as we have it here. For many tasks, such as audio signal processing, the dataset consists of smaller audio signals, which can be processed individually. Thus, an incremental training method was implemented in PyRCN. This makes it possible to train at least smaller ESNs on a fairly modern computer efficiently.

To optimize the hyper-parameters, at first, we fix $K^{\text{in}} = K^{\text{rec}} = 10$ in order to have sparse input-to-reservoir and reservoir-to-reservoir connections. Furthermore, we fixed the reservoir size to $N^{\text{res}} = 500$, because optimizing the hyper-parameters for this task is still computationally expensive, due to the large amount of data. We have seen that the input scaling α_u and the spectral radius ρ are interacting to optimize the trade-off between current and past information. Thus, we perform a grid search over those two hyper-parameters (ranges 0 to 1, step 0.1) and report the MSE on the training set for each parameter combination, while we did not use bias or leaky integration. The best hyper-parameters were $\alpha_u = 0.6$ and $\rho = 0.2$. Next, we wanted to determine the ideal stable states for each reservoir neuron. Thus, we optimized the bias scaling α_b with the fixed hyper-parameters $\alpha_u = 0.6$ and $\rho = 0.2$. This led to $\alpha_b = 0.7$. Finally, we optimized the leakage, which is a more global hyper-parameter, because it affects every reservoir neuron in the same way. In this case, $\lambda = 0.3$ was the most suitable value.

Fig. 9 shows the impulse responses of the reservoir neurons for a strongly simplified ESN. We used the same hyper-parameters but a one-dimensional input. We can see that the impulse responses have a duration of around 15 samples and are rather smooth due to the low leakage. The mean note duration in the MusicNet is 0.2 s. Thus, given a frame rate of 100 Hz, the output labels are constant for 20 frames on average. Thus, we can observe that the duration of all impulse responses is long enough to capture most of the output dynamics.

For the actual recognition result, we report Precision P , Recall R and F -Measure for different reservoir sizes in Table I. It can be noticed that both increasing the reservoir sizes and introducing bidirectional reservoirs improves the results significantly. The current state of the art, a CNN [18], was

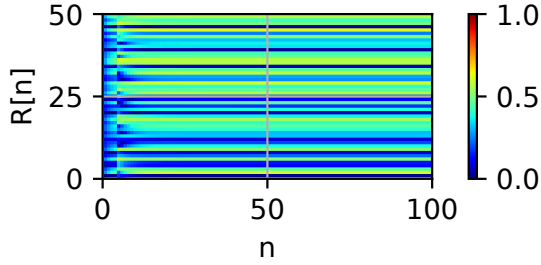


Fig. 9: Impulse responses for the ESN utilized for multipitch tracking. They have a duration of around 15 samples and have rather smooth trajectories, due to the low leakage.

not outperformed. However, in this paper, we have restricted the reservoir size for the purpose of demonstrations. Thus, our best model has significantly less (1024 128) trainable parameters than the reference (26 132 480) model. As we have not yet noticed overfitting of the ESN model, it could be further increased and additional layers added on top of this architecture.

TABLE I: Results of the ESN for multipitch tracking using different reservoir sizes. More neurons always improved the performance of the ESN. Introducing bi-directional reservoirs also improved the results significantly. Comparing to one reference method, we have not outperformed the CNN proposed in [18].

Model	P	uni		P	bi	
		R	F		R	F
500	0.52	0.66	0.5770	0.56	0.74	0.64
1000	0.53	0.67	0.59	0.57	0.76	0.65
2000	0.54	0.69	0.61	0.59	0.77	0.67
4000	0.58	0.70	0.62	0.60	0.79	0.68
CNN [18]				0.70	0.76	0.73

B. Spoken Digit Recognition

The application of ESNs for speech recognition tasks has been investigated in detail in [2], [14]. In this section we adopt a simple sub task of that work to study the robustness of multi-layer ESNs and their capability to adapt to unseen conditions.

All experiments are conducted on the Aurora-2 database [19]. This database contains clean and noisy utterances, sampled at 8 kHz and filtered with a G712/MIRS characteristic. The vocabulary consists of the digits 0 to 9 and the letter 'o' that is a pronunciation variant of "zero". There are 8440 clean training samples, 2412 of which contain only one digit. The Aurora-2 dataset also provides noisy versions of the recorded data by artificially adding noise to the clean samples at Signal-to-Noise Ratios (SNR) between 20 and -5dB. We have selected 500 isolated digit samples from the training set and split them into sets of 375 and 125 samples for training and validation, respectively. we report the digit error rate (DER), which is the

ratio of the wrongly classified samples to the total number of samples in the validation set.

Each sample is labeled with the corresponding digit. However, the silence parts and the beginning and end time of the digits are not annotated. If we label all the frames of each sample as its labeled digit, the silence parts may hamper the performance of the model. Therefore one of the challenges would be to find the digit boundaries in the recorded sample.

The acoustic features extracted from the input signal are MFCCs (plus log-energy) and their first and second derivatives. The output classes are the eleven digits (including the variants *zero* and *oh* for digit 0) and *silence*. During training, each frame was associated with one of these classes. The silence frames at the beginning and the end of the utterance were delimited using a simple energy-based silence detector. This detector used a decision threshold that was given by

$$E^{\text{thr}} = (1 + a) \min(\hat{\mathbf{E}}) + b \max(\hat{\mathbf{E}}), \quad (5)$$

with $a = 0.6$ and $b = 0.1$ being two control parameters tuned empirically on the training set and with $\hat{\mathbf{E}}$ being the frame energy that was obtained by smoothing the frame-wise energies. During the evaluation, we consider the digit class with the highest accumulated output as the recognized digit.

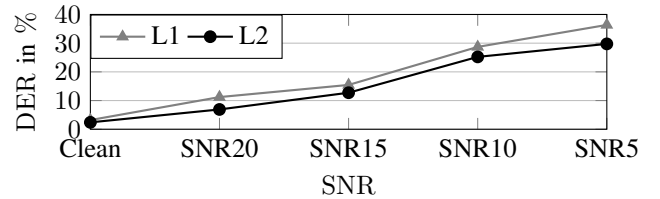


Fig. 10: Performance of a 2-layer ESN with 2K and 1K neurons respectively. The model is trained on clean samples and tested on various noise levels of the validation set.

Fig. 10 shows the performance of a two layer ESN with 2000 and 1000 neurons in the first and second layer, respectively. The models has been trained on clean data only but has been evaluated on various levels of noise from clean to SNR5. Also the second layer has been supplied with the readouts of the first layer. According to this figure the main contribution of the second layer is to learn and correct the error patterns made by the first layer.

For instance in Fig. 11, we observe how the second layer corrects the output of the first layer for a recorded audio of digit 4 with SNR15.

Injecting some noisy data during the training phase can improve the robustness of a machine learning model. We consider three scenarios:

- 1) *multi*: In which both layers are trained with the clean and noisy versions of the training data (Clean, SNR20 and SNR15)
- 2) *multi-L2*: In which the first layer is trained with clean data while second layer is trained with clean and noisy training samples as mentioned above.

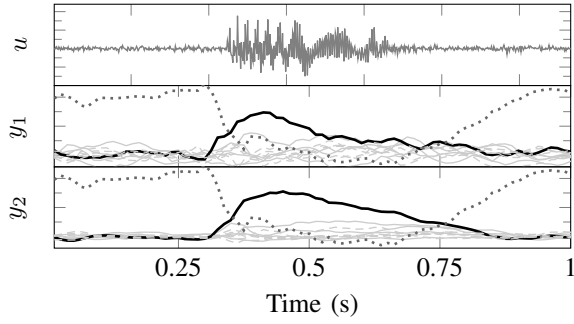


Fig. 11: Example of an input audio for a spoken digit “4” with SNR15 and the readouts of the first and second layer of an ESN trained on clean data. The bold black and the dotted lines belongs to the readout for digit 4 silence, respectively.

- 3) *adapt*: Both layers are trained with the combination of the clean samples of the training set along with the clean, SNR20 and SNR15 samples of the validation set.

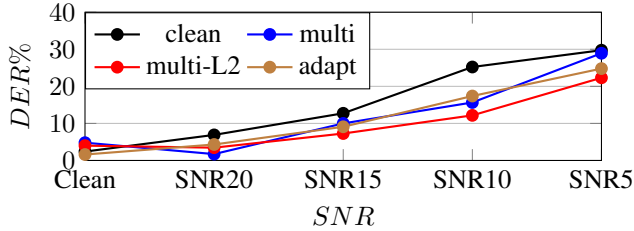


Fig. 12: Comparing different scenarios to improve the robustness of ESNs in noisy conditions.

According to Fig. 12 and for this specific task, it is more beneficial to let the first layer learn the clean environment and train only the second layer on both clean and noisy data. An interesting observation is the comparison between *multi-L2* and *adapt*: although the latter benefits from adapting to some validation samples, the *multi-L2* which has solely been trained on training samples (layer 1 on clean and layer 2 on noisy versions). This can confirm that the ESN benefits more from learning the noise patterns rather than seeing the new samples.

VI. CONCLUSION AND OUTLOOK

We presented PyRCN, a new Python toolbox for ESNs with a scikit-learn interface. It is relatively light-weight and allows convenient hyper-parameter optimization. Using the toolbox, we have analyzed the impact of different hyper-parameters on impulse responses of reservoir neurons. We have also proposed different use-cases from classification to regression to show the wide range the toolbox can be used for. In the future, we will continue to work on further optimizations of the underlying methods of the toolbox and consider exposing additional interfaces to support other established machine learning frameworks, e.g., PyTorch or Keras. We strongly encourage the interested reader to try out the toolbox and welcome and appreciate any feedback.

REFERENCES

- [1] H. Jaeger, “The “echo state” approach to analysing and training recurrent neural networks,” German National Research Center for Information Technology, Tech. Rep. GMD Report 148, 2001. [Online]. Available: <http://www.faculty.iu-bremen.de/hjaeger/pubs/EchoStatesTechRep.pdf>
- [2] F. Triefenbach, A. Jalalvand, K. Demuynck, and J.-P. Martens, “Acoustic modeling with hierarchical reservoirs,” *IEEE Transactions on Audio, Speech, and Language Processing*, vol. 21, no. 11, pp. 2439–2450, 2013.
- [3] A. Jalalvand, K. Demuynck, W. D. Neve, and J.-P. Martens, “On the application of reservoir computing networks for noisy image recognition,” *Neurocomputing*, vol. 277, pp. 237 – 248, 2018.
- [4] A. Jalalvand, B. Vandersmissen, W. D. Neve, and E. Mannens, “Radar signal processing for human identification by means of reservoir computing networks,” in *IEEE Radar Conference*. IEEE, 2019, pp. 1–6.
- [5] P. Steiner, S. Stone, P. Birkholz, and A. Jalalvand, “Multipitch tracking in music signals using echo state networks,” in *28th European Signal Processing Conference (EUSIPCO)*, 2020, 2020, accepted.
- [6] M. Lukoševičius, *A Practical Guide to Applying Echo State Networks*. Berlin, Heidelberg: Springer Berlin Heidelberg, 2012, pp. 659–686.
- [7] J. B. Mockus and L. J. Mockus, “Bayesian approach to global optimization and application to multiobjective and constrained problems,” *Journal of Optimization Theory and Applications*, vol. 70, no. 1, pp. 157 – 172, Jul 1991.
- [8] H. Jaeger, “Adaptive nonlinear system identification with echo state networks,” in *Advances in Neural Information Processing Systems 15*, S. Becker, S. Thrun, and K. Obermayer, Eds. MIT Press, 2003, pp. 609–616. [Online]. Available: <http://papers.nips.cc/paper/2318-adaptive-nonlinear-system-identification-with-echo-state-networks.pdf>
- [9] C. Gallicchio, A. Micheli, and L. Pedrelli, “Deep reservoir computing: A critical experimental analysis,” *Neurocomputing*, vol. 268, pp. 87 – 99, 2017, advances in artificial neural networks, machine learning and computational intelligence. [Online]. Available: <http://www.sciencedirect.com/science/article/pii/S0925231217307567>
- [10] D. Verstraeten, B. Schrauwen, S. Dieleman, P. Brakel, P. Buteneers, and D. Pecevski, “Oger: modular learning architectures for large-scale sequential processing,” *Journal of Machine Learning Research*, vol. 13, pp. 2995–2998, 2012.
- [11] N. Trouvain, L. Pedrelli, T. T. Dinh, and X. Hinaut, “ReservoirPy: an Efficient and User-Friendly Library to Design Echo State Networks,” May 2020, working paper or preprint. [Online]. Available: <https://hal.inria.fr/hal-02595026>
- [12] N. Schaetti, “EchoTorch: Reservoir computing with PyTorch,” <https://github.com/nschaetti/EchoTorch>, 2018.
- [13] F. Pedregosa, G. Varoquaux, A. Gramfort, V. Michel, B. Thirion, O. Grisel, M. Blondel, P. Prettenhofer, R. Weiss, V. Dubourg, J. Vanderplas, A. Passos, D. Cournapeau, M. Brucher, M. Perrot, and E. Duchesnay, “Scikit-learn: Machine learning in Python,” *Journal of Machine Learning Research*, vol. 12, pp. 2825–2830, 2011.
- [14] A. Jalalvand, F. Triefenbach, K. Demuynck, and J.-P. Martens, “Robust continuous digit recognition using reservoir computing,” *Computer Speech & Language*, vol. 30, no. 1, pp. 135 – 158, 2015.
- [15] H. Jaeger, M. Lukoševičius, D. Popovici, and U. Siewert, “Optimization and applications of echo state networks with leaky- integrator neurons,” *Neural Networks*, vol. 20, no. 3, pp. 335 – 352, 2007, echo State Networks and Liquid State Machines.
- [16] Z. Zhao, H. Liu, and T. Fingscheidt, “Nonlinear prediction of speech by echo state networks,” in *26th European Signal Processing Conference (EUSIPCO)*, 2018, 2018, pp. 2085–2089.
- [17] X. Lin, Z. Yang, and Y. Song, “Short-term stock price prediction based on echo state networks,” *Expert Systems with Applications*, vol. 36, no. 3, Part 2, pp. 7313 – 7317, 2009.
- [18] J. Thickstun, Z. Harchaoui, D. P. Foster, and S. M. Kakade, “Invariances and data augmentation for supervised music transcription,” in *2018 IEEE International Conference on Acoustics, Speech and Signal Processing (ICASSP)*, April 2018, pp. 2241 – 2245.
- [19] H.-G. Hirsch and D. Pearce, “The AURORA experimental framework for the performance evaluation of speech recognition systems under noise conditions,” in *Automatic Speech Recognition: Challenges for the Next Millennium*. ISCA ITRW, 2000, pp. 181–188.